

Encapsulation and Release of Cladribine from Chitosan Nanoparticles

Rachel E. Domaratzki, Amyl Ghanem

Chemical Engineering Program, Department of Process Engineering and Applied Sciences, Dalhousie University, Halifax, Nova Scotia, Canada B3J 2X4

Correspondence to: A. Ghanem (E-mail: amyl.ghanem@dal.ca)

ABSTRACT: This study shows the potential of chitosan (CH) nanoparticles as both an oral and IV drug delivery system using the anticancer drug cladribine as a model drug. Smooth, spherical nanoparticles were prepared by the ionotropic gelation of CH with sodium tripolyphosphate. Nanoparticle size depended on degree of hydration, drug loading, and crosslinking conditions, with the smallest nanoparticles in the size range of 212 ± 51 nm. Cladribine was entrapped in the CH matrix with an entrapment efficiency of up to 62%, depending on the initial loading. The release of cladribine followed a near-Fickian diffusion rate over the first several hours and then reached a plateau. A second release phase began after 30–40 h of incubation in the release medium, and proceeded until ~ 100 h. Loaded CH nanoparticles that were crosslinked with genipin showed a delayed release profile, with only 40% of loaded drug being released after 100 h. © 2012 Wiley Periodicals, Inc. *J. Appl. Polym. Sci.* 000: 000–000, 2012

KEYWORDS: biomaterials; drug delivery systems; interpenetrating networks (IPN); microencapsulation; nanoparticles; nanowires and nanocrystals

Received 11 June 2011; accepted 18 July 2012; published online

DOI: 10.1002/app.38354

INTRODUCTION

In recent years, biodegradable biopolymers have attracted increasing attention as potential drug delivery systems (DDSs). Polymeric nanoparticles used for drug delivery have advantages over other DDSs due to their increased uptake by cells, higher entrapment efficiencies, and increased stability.¹ Polymers that have been used for nanoparticle DDSs include poly(lactide), poly(lactide-co-glycolide) (PLGA), polycaprolactone, and natural polymers such as chitosan (CH), gelatin, and alginate.²

CH is a naturally occurring, high molecular weight, cationic polysaccharide derived from crustacean shells and is generally biocompatible and biodegradable. CH has several unique properties that are advantageous for DDSs. It has been reported that CH is mucoadhesive and also enhances the mucosal barrier permeability.^{3,4} These properties may enhance uptake of an orally administered drug. CH nanoparticles will form under mild processing conditions (room temperature, atmospheric pressure, no organic solvents), permitting incorporation of biologically active molecules during processing. Many polymer nanoparticle formation methods require complex processing steps and organic solvents that may damage sensitive molecules. The hydroxyl groups and reactive amino group of CH can easily be modified under mild reaction conditions (room temperature, atmospheric pressure, no organic solvents) to add functional groups and provide molecule specificity.

Cladribine (CdA, 2-chloro-2'-deoxyadenosine) is a nucleoside analogue primarily used in the treatment of hairy cell leukemia and B-cell chronic lymphocytic leukemia,⁵ and recently as a treatment for multiple sclerosis. Cladribine and other nucleoside analogue drugs are administered in high IV doses due to their rapid clearance from the bloodstream. However, high doses of CdA have cytotoxic effects on resting and proliferating cells, and can temporarily weaken the immune system.⁶ CdA is typically administered by either continuous intravenous infusion that extends over a week or daily 2-h infusions over 5 days.⁵ This form of drug administration often results in patient discomfort, adverse side effects due to fluctuations in plasma drug concentration, and severe toxic side effects.⁶ A nanoparticle DDS would help to protect cladribine from degradation in the bloodstream for IV dosage regimes, permitting administration of lower doses. This type of a system may also serve as a basis for the development of an oral chemotherapeutic formulation. Cladribine is useful as a drug model for other purine antimetabolites. Methods developed in the drug delivery of cladribine would also be useful in the delivery of other drugs that are easily degraded *in vivo*.

In this research, cladribine was incorporated into CH nanoparticles by two methods: (1) entrapment during gelation or (2) entrapment during gelation followed by crosslinking of the CH matrix. Two novel crosslinking agents were used, genipin or

glyoxal, as a less toxic alternative to the more traditionally used crosslinker glutaraldehyde. Genipin is extracted from fruit of the plant *Gardenia jasminoides* Ellis, Genipin is up to 10,000 times less cytotoxic than glutaraldehyde.⁷ Genipin crosslinked CH and CH derivatives have also been investigated for drug release applications. Mi et al. investigated the use of genipin in indomethacin-loaded CH beads and found that drug release was slow and constant.⁷ CH nanoparticles are formed in the presence of sodium tripolyphosphate (TPP) by ionotropic gelation. When a drug is present during gelation, it is contained between the ionically crosslinked CH molecules. The CH nanoparticle protects the entrapped drug from degradation and modulates its release rate. Drug is released by diffusion through the matrix and then via degradation of the nanoparticle. When drug entrapment is followed by crosslinking (e.g., with genipin), additional covalent crosslinking bonds are formed on the outside of the nanoparticle matrix, which may decrease the rate of diffusion and degradation, thereby slowing drug release. The use of a covalent crosslinker such as genipin may alter drug release properties of CH nanoparticles.

EXPERIMENTAL

Materials

CH with 80, 90, and 100% degrees of deacetylation (DDA) was purchased from Carbomer (San Diego, CA). All other chemicals were of analytical grade from Sigma-Aldrich (St. Louis, MO).

Preparation of Chitosan Nanoparticles

CH nanoparticles were formed by the dropwise addition of TPP solution (1 mg/mL) to CH (1 mg/mL in acetic acid) in a 1–5 volume ratio. The mixture was stirred gently for 1 min at room temperature to form nanoparticles. The mixture was then centrifuged for 120 min at $1200 \times g$ and the supernatant removed.⁸ For immediate use of fresh nanoparticles, the pellet was resuspended in 0.5 mL of deionized water.

Preparation of Cladribine Loaded Chitosan Nanoparticles

The cladribine-loaded CH nanoparticles were prepared by adding cladribine to the TPP solution before nanoparticle formation in loading quantities of 1, 5, or 10% (w/w) with respect to initial CH mass. The nanoparticles were prepared as in the previous paragraph. The supernatant was removed and analyzed for cladribine concentration, whereas the nanoparticles in the pellet were resuspended in deionized water for application.

Preparation of Crosslinked Nanoparticles

Cladribine-loaded CH nanoparticle samples were first prepared as described in the previous paragraph. Immediately after preparation, the loaded nanoparticles were then crosslinked by incubation in 2 mL of crosslinking solution (50 mg/mL glyoxal or 0.1 mg/mL genipin) under constant stirring for a reaction time of 2 h.

Measurement of Cladribine Concentration

The cladribine concentration in the supernatant samples was determined based on the absorbance of the samples at 265 nm.⁹ Supernatant samples from nanoparticles made with 5 and 10% initial cladribine loadings were diluted 1 : 10 with dH₂O in order to bring the absorbance within the limits of the assay. Sample absorbances were measured in 1.7 mL quartz cuvettes, using a Shimadzu UV-1700 Pharma Spec UV–visible Spectro-

photometer (Suzhou, Jiangsu, China). A standard curve was prepared by diluting cladribine in a solution of 1 : 10 blank supernatant in dH₂O. Good linearity was observed, and this method was validated using high performance liquid chromatography (HPLC). The amount of cladribine entrapped in the nanoparticle was determined by subtracting the cladribine measured in the supernatant from the known initial loading.

Characterization of Chitosan Nanoparticles

The size of the nanoparticles and the polydispersity index of each sample were determined using dynamic light scattering (DLS) on a Brookhaven 90Plus Particle Size Analyzer (Brookhaven, NY). Samples were measured after 1 min autocorrelation and five runs were performed on each sample. The samples were measured at 20°C, angle of 90°, and volume of 1 mL.

The morphology and size of the nanoparticles (air dried) were evaluated using a Philips Tecnai 12 transmission electron microscope (TEM; Eindhoven, The Netherlands). Samples were mounted on Formvar-coated copper grids, negatively stained with 2% phosphotungstic acid, and allowed to dry. This method was used to measure size of 0%, 1%, 5%, and 10% loaded nanoparticles. Nanoparticles were incubated in phosphate buffered saline (PBS) (pH 7.4) or lysozyme (10 µg/mL) for 24 and 100 h and then observed by TEM.

Determination of Cladribine Entrapment Efficiency and Loading Capacity

Entrapment efficiency describes the quantity of the drug entrapped within the nanoparticle compared with the initial drug loading, and was determined according to the following equation:

$$EE = \frac{m_e}{m_i} \times 100 \quad (1)$$

where EE is an entrapment efficiency (%), m_e is mass of drug entrapped in nanoparticles (µg), and m_i is mass of initial drug loading (µg).

The mass of drug entrapped in the nanoparticles is determined by subtracting the quantity of drug remaining in the supernatant after entrapment from the amount of drug initially added to the nanoparticles.¹

The loading capacity describes the percentage of the total nanoparticle mass, which can be attributed to the mass of the entrapped drug. The mass of cladribine-loaded nanoparticle samples was determined after air-drying the samples.

$$LC = \frac{m_e}{m_n} \times 100 \quad (2)$$

where LC is loading capacity (%), m_e is mass of drug entrapped in nanoparticles (µg), and m_n is total mass of cladribine loaded nanoparticles (µg).

Cladribine Release from Chitosan Nanoparticles

The cladribine-loaded nanoparticles were incubated under stirring (100 rpm) in 25 mL of release medium (PBS pH 7.4 unless otherwise indicated) to monitor the amount of cladribine released from the nanoparticles over time. One milliliter

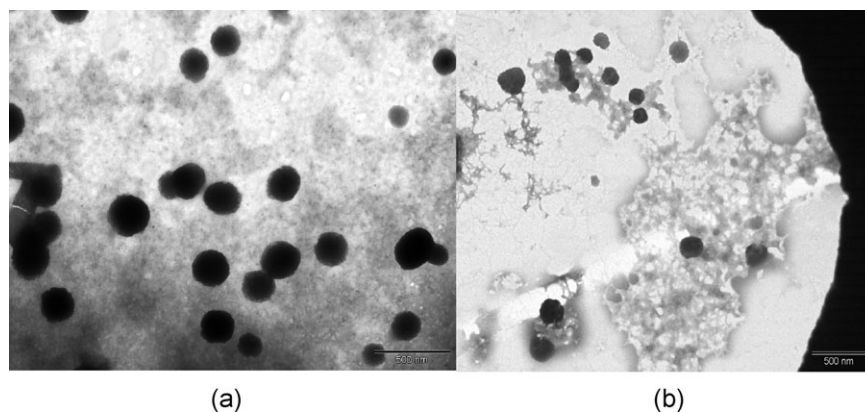


Figure 1. Chitosan nanoparticles (a) and cladribine-loaded chitosan nanoparticles (b).

samples of release media were removed at selected time points and the cladribine concentration was analyzed by UV spectroscopy as described above. To avoid the presence of nanoparticles in the release media, the cladribine-loaded nanoparticles were first placed into dialysis tubing (Spectra/Por 1 MWCO 6000–8000), which was then suspended in the release medium.¹⁰

Statistics

Experiments were all conducted in triplicate or more. All data are given as the mean of a minimum of three samples \pm standard deviation, unless otherwise indicated. Statistical significance was determined by Student's *t*-test or ANOVA where applicable, with $\alpha = 0.05$ denoting significance.

RESULTS

Characterization of Chitosan Nanoparticles

Nanoparticle formation was successfully accomplished by ionic gelation of CH with TPP and was observed visually by the instantaneous formation of an opalescent solution. Based on the work of Zhang et al.,⁸ CH to TPP ratio of 5 : 1 was used. Confirmation of nanoparticle formation was evident from the TEM images that showed distinct, spherical particles with smooth edges as seen in Figure 1(a).

The size of the freshly prepared hydrated nanoparticles and the air dried nanoparticles were measured and compared. The average diameter of hydrated, unloaded 90% DDA CH nanoparticles was found to be 923 ± 125 nm ($n = 393$). These unloaded nanoparticles made under same conditions were air dried and characterized using TEM. The average diameter of the unloaded air dried nanoparticles was 212 ± 51 nm ($n = 146$), a 77% decrease from their freshly prepared size. This amount of particle shrinkage can be attributed to the large amount of water that is contained in the particle matrix, which is removed upon drying. The particles remain smooth and spherical upon drying, and drying can be used as a means to reduce the particle size.

Incorporation of cladribine into the CH nanoparticles resulted in the formation of an opalescent solution similar to the unloaded CH nanoparticles. A TEM image of the cladribine loaded nanoparticles is shown in Figure 1(b). The morphology continues to be spherical; however, the edges are not as smooth as the unloaded nanoparticles. The average diameters of the fresh 1, 5, and 10%

cladribine-loaded nanoparticles were 636 ± 13 ($n = 327$), 812 ± 93 ($n = 376$), and 820 ± 110 ($n = 354$), respectively. The loaded nanoparticles are smaller in size compared with the unloaded nanoparticles, suggesting that the presence of the drug increased the strength of the ionic bonds. Alternatively, the cladribine may contribute to the number of positive sites available for interaction with TPP, further contracting the matrix. However, the sizes increased with increasing drug loading, due to the added bulk of the drug. When dried, the nanoparticle size was determined by TEM to be 414 ± 124 nm ($n = 24, 5,$ and 10% initial loading). The nanoparticles decreased 51% in size upon drying, exhibiting less shrinkage compared with unloaded particles due to the addition of cladribine, which remains in the structure after drying, unlike water. The rough edges of the particles may be due to the presence of drug molecules at the surface.

Cladribine Entrapment and Loading in Nanoparticles

The method of drug incorporation had a significant effect on the entrapment efficiency and loading capacity of cladribine in CH nanoparticles. When cladribine was added first to the TPP solution (pH 9.0), entrapment efficiency was $62.2 \pm 5.4\%$ for a 1% initial cladribine loading (w/w with respect to initial CH solution). However, when the 1% initial loading cladribine-entrapped nanoparticles were prepared by adding a CH-cladribine solution to a TPP solution, entrapment efficiency fell significantly to $16.8 \pm 8.6\%$. This is likely due to the ionic interaction between positive CH and positive cladribine. The first method was used in subsequent experiments.

The entrapment efficiency and loading capacity was not affected by the DDA of the CH, holding all other parameters constant (data not shown). Subsequent experiments were conducted using CH with a 90% DDA. The effect of initial loading on entrapment efficiency and loading capacity are reported in Figure 2(a, b). For the 1, 5, and 10% initial cladribine loadings, the entrapment efficiency was 62.2 ± 8.6 , 20.3 ± 1.1 , and $20.3 \pm 4.5\%$, respectively. The loading capacities for 1, 5, and 10% initial cladribine loadings were 2.5 ± 0.35 , 4.1 ± 0.23 , and $8.3 \pm 1.8\%$, respectively. Loading capacity increased with initial loading due to a larger quantity of drug present in the particles, whereas the entrapment efficiencies decreased with initial loading indicating that a lower percentage of the total drug added actually ended up in the nanoparticle and that the process

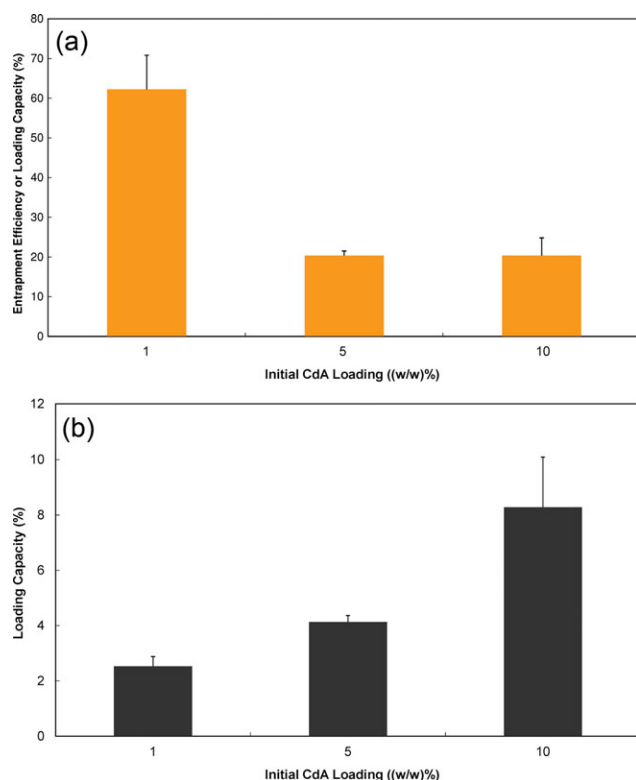


Figure 2. Entrapment efficiency (a) and loading capacity (b) vary with initial cladribine loading. Mean \pm standard deviation, $n = 3$. [Color figure can be viewed in the online issue, which is available at wileyonlinelibrary.com.]

becomes less efficient as the amount of drug added increases. The loading capacity continues to increase as initial loading is increased to 10%, indicating that the maximum particle loading has not yet been reached. For the release experiments, nanoparticles were made with 10% initial loading conditions, 90% DDA as they had the largest total drug loading of nanoparticles made in this study.

Cladribine Release from Chitosan Nanoparticles

The release profile of cladribine-loaded nanoparticles was measured and is shown in Figure 3. The profile is biphasic, consisting of an initial release phase, a plateau, and a second release phase. Complete release of the cladribine is measured. In the first 6 h, 38% of the entrapped cladribine was released from the nanoparticles, which corresponds to 10 μg of cladribine. The plateau phase occurred from 6 to 30 h after incubation, during which no cladribine release was measured. The second phase of cladribine release began again at 30–40 h after initial incubation, and 100% of the entrapped cladribine was released by 80 h. The shapes of the release curves are distinctly different for the two release periods, indicating that different mechanisms may be controlling the release in the two time periods.

Drug release from polymer matrices can occur due to several mechanisms. The drug is presumed to be entrapped in a matrix, confined by the ionic crosslinks formed by the CH and the TPP. Drug molecules located near the surface may diffuse to the bulk fluid, this is, usually considered the “burst” release evidenced by

a high initial concentration of drug measured in the early time period. Drug that is entrapped in the bulk of the polymer may diffuse out more slowly, this diffusion is enhanced if the polymer matrix swells, increasing the size of the pores for drug to diffuse through. Erosion and degradation of the matrix can occur, causing a release of the drug and matrix molecules to the bulk fluid. These mechanisms can occur alone or together. It is possible that the two-phase release observed in these experiments can be explained by the progression of different release mechanisms, with a delay in transition between the mechanisms giving a “plateau” phase.

Cladribine Release from Crosslinked Nanoparticles

Genipin is a natural crosslinking agent obtained from the fruits of the plant *Gardenia jasminoides* Ellis and is reported to be less toxic than glutaraldehyde and therefore appropriate for clinical applications.¹¹ Crosslinking between genipin and CH occurs by the formation of a secondary amide bond between the amino groups of CH and the ester groups of genipin.¹² When glyoxal is used as a crosslinking agent, imide bonds between the glyoxal aldehyde groups and the CH amine groups are expected to be formed.

The CH nanoparticles were covalently crosslinked after cladribine entrapment with the intention of modulating the drug release, particularly in the initial time period where a burst release is observed. The drug release profiles from crosslinked nanoparticles were then measured as described in the “Experimental” section and are shown in Figure 4.

The initial release of cladribine from both genipin (90% DDA) and glyoxal (100% DDA) crosslinked nanoparticles was low with a small burst release taking place in the first 3 h showing $\sim 8\%$ release from genipin and 4% from glyoxal. This low initial release (compared with the ionically crosslinked particles) could be due to slower diffusion caused by increased crosslinking density of the surface.

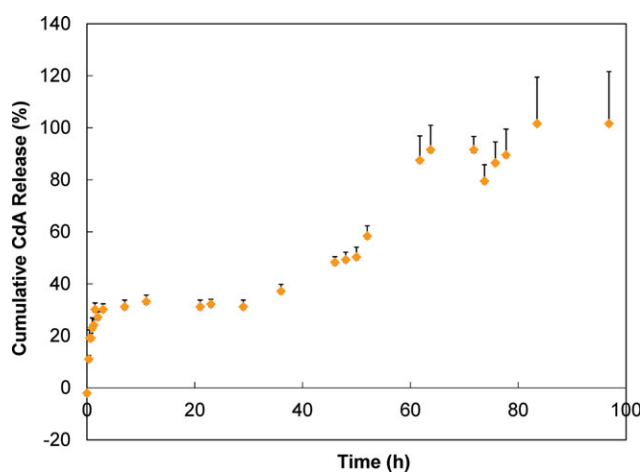


Figure 3. Cladribine release from 10% initial CdA loading entrapped nanoparticles into PBS, pH 7.4 (90% DDA CH, 20.4 μg cladribine). Mean \pm standard deviation, $n = 3$. [Color figure can be viewed in the online issue, which is available at wileyonlinelibrary.com.]

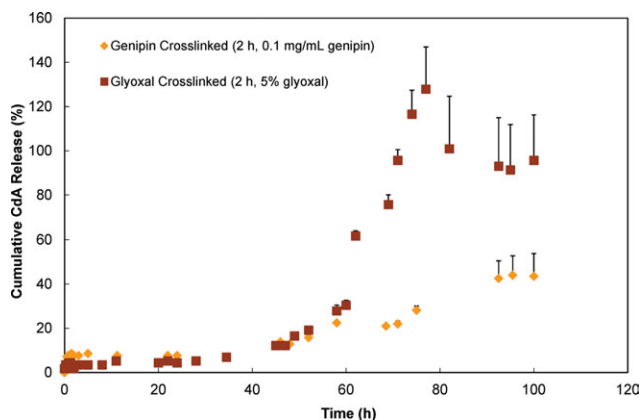


Figure 4. Overall release from crosslinked cladribine-loaded nanoparticles into PBS, pH 7.4. Mean \pm standard deviation, $n = 3$. [Color figure can be viewed in the online issue, which is available at wileyonlinelibrary.com.]

The burst release phase was followed by a long plateau phase where no drug was released. Drug release started again for both types of crosslinked nanoparticles at 50 h; however, the rate of release differed. From 50 h to 100 h, the glyoxal crosslinked particles released cladribine more rapidly compared with genipin crosslinked particles. After 100 h, all of the cladribine entrapped in the glyoxal crosslinked nanoparticles was released ($100 \pm 44\%$). The glyoxal crosslinked particles released the same total amount of cladribine at the same final release time as the ionically crosslinked nanoparticles, indicating that the glyoxal crosslinking did not have an effect on the final cumulative release, but the time at which most of the cladribine was released was delayed.

The genipin crosslinked nanoparticles showed a similar release profile to the glyoxal crosslinked nanoparticles for the first 50 h. From 50 to 100 h, the rate of drug release from the genipin crosslinked nanoparticles was lower than that from both the ionically crosslinked and glyoxal crosslinked nanoparticles. After 100 h, only $43 \pm 16\%$ of the initially entrapped cladribine was released, suggesting that cladribine still remains entrapped within the genipin crosslinked matrix after 100 h. It is hypothesized that the second phase of release is due to particle degradation, and the strength of crosslinking of the genipin leads to less CH matrix degradation. This slower release rate could be advantageous in situations where a longer release period is desired. Also, the shape of the release profile is distinctly more linear than the glyoxal and ionically crosslinked nanoparticles, which is also a preferable release profile. The results shown here are from only one set of crosslinking conditions. Under different genipin concentrations or crosslinking times, the degree of crosslinking by genipin could be manipulated thereby adjusting the release rate.

Crosslinking of the nanoparticles reduced their overall size. DLS measurement of unloaded, genipin crosslinked nanoparticles indicated an average particle diameter of 560 nm ($n = 65$), compared with an unloaded, ionically crosslinked nanoparticle size of 923 nm ($n = 393$). Genipin crosslinking tightened the surface of the matrix in the process of creating covalent bonds.

Nanoparticle Degradation

Controlled release of drugs from nanoparticles may occur due to degradation of the nanoparticle itself. It is likely that the release of

at least some of the cladribine entrapped in the CH nanoparticles is from degradation of the CH nanoparticle matrix, particularly during the second release phase. In a preliminary investigation, nanoparticles were incubated in either PBS (pH 7.4) or lysozyme ($10 \mu\text{g/mL}$) for 24 and 100 h. Lysozyme is an enzyme known to degrade the CH nanoparticle matrix. TEM images were used to monitor nanoparticle size and morphology after incubation. Nanoparticle diameter decreased significantly when incubated in either solution for 100 h as shown in Figure 5. A decrease in diameter is indicative of surface erosion of the CH matrix, causing gradual release of the entrapped drug and an increase in drug diffusion due to reduced matrix density. The onset of degradation could be responsible for the second release phase.

Application of Mathematical Models to Cladribine Release

Mathematical equations can be used to describe the release rate of drugs from the matrix to elucidate the mechanism of release and to predict release rates. The most comprehensive semi-empirical equation used to describe drug release from polymeric systems is the Power Law model.^{13,14}

$$\frac{M(t)}{M_{\infty}} = kt^n$$

where M_t and M_{∞} are the cumulative amount of drug released at time t and infinite time, respectively; k is the apparent release rate constant (min^{-n}) and n is the release exponent, indicative of the mechanism of drug release. Experimental release data up to the first 60% of fractional release is fit to this equation and constants are determined. When the geometry of the delivery system is spherical, a release exponent n of 0.43 indicates that Fickian diffusion is the controlling release mechanism, $0.43 < n < 0.85$ indicates anomalous transport, and $0.85 < n$ indicates Type II transport. The cladribine release data (shown in Table I) from ionically crosslinked, glyoxal crosslinked, and genipin crosslinked nanoparticles was fit to the Power Law model. The data for cladribine release from ionically crosslinked nanoparticles follows two distinct phases, an initial release phase and a second release phase. The initial release phase data fit the model well ($R^2 > 0.9$)

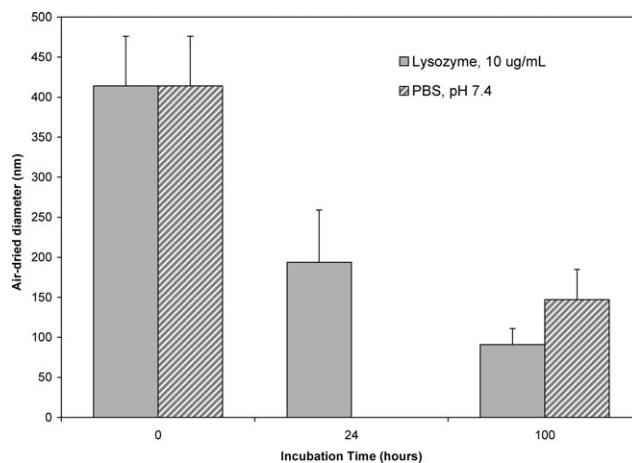


Figure 5. Size of 10% initial cladribine loading nanoparticles after incubation in various media. Mean \pm standard deviation, $n = 3$.

Table I. Power Law Constants

	n	End of phase 1 (min)	Start of phase 2 (h)	n
Ionically crosslinked	0.56	120	36	1.65
Glyoxal crosslinked	0.43	120	46	4.80
Genipin crosslinked	1.10	30	45	1.59

giving a Power Law release exponent n in the range of 0.22–0.45 (depending on release medium) indicative of Fickian diffusion.^{15,16} This indicates that the release of cladribine from ionically crosslinked CH nanoparticles in the first phase follows Fickian diffusion. The cladribine release data from glyoxal crosslinked nanoparticles also gave a release exponent in the Fickian diffusion range; however, as the fit was poor ($R^2 = 0.46$), no conclusions will be drawn. The genipin crosslinked nanoparticles in this initial phase time period did not fit the Power Law model.

DISCUSSION

The development of many promising new drugs is often abandoned due to problems with drug stability, solubility, or difficulty maintaining a therapeutic drug concentration. DDSs like CH nanoparticles are developed to alleviate these problems by protecting or carrying the drug, and providing a sustained release. Cladribine and other nucleoside analogs have short half-lives in circulation due to rapid degradation by enzymes and, therefore, are administered in high doses that may lead to severe toxic effects. By incorporating the drug into a CH nanoparticle that protects the drug from degradation, it may be possible to administer lower doses thereby preventing toxic effects while still achieving efficacy.

The size of the DDS is an important factor, with different size ranges optimal for oral or IV administration. The size range of the CH nanoparticles made in this study varied with state of hydration and the presence of cladribine. Nanoparticles with sizes as low as 212 (air dried) and up to 1000 nm (hydrated) were made in this study. Previous researchers indicate that the optimal nanoparticle size for IV delivery is 100 nm. It has also been shown that endocytosis of particles smaller than 500 nm may facilitate transport of anticancer drugs across the intestinal barrier making them suitable for oral drug delivery vehicles.¹⁷ Particle uptake into CaCo₂ cells (an established *in vitro* model for investigation of transport across the intestinal epithelium) showed that particle uptake was greatest in the 100–200 nm size; however, particles in the 500 nm and 1000 nm range were also taken up by cells at a lower rate.¹⁶ Therefore, the nanoparticles produced by this method (with the inclusion of cladribine, and air dried) are of an appropriate size for passage through the intestinal barrier and oral delivery, and close to the threshold for optimal IV delivery.

The entrapment efficiency varied significantly with the initial loading of cladribine [ranging from 62.2% to 20.3% (1% initial loading to 10% initial loading)]. This is in the same range as

other methods of drug incorporation into CH delivery matrices. Insulin was entrapped into CH nanoparticles with 75–80% efficiency,¹⁸ tetanus toxoid entrapped with 50% efficiency,¹⁹ retinol entrapped with 65% efficiency,¹⁵ and bovine serum albumin (BSA) entrapped with up to 79% depending on BSA : CH ratio.¹⁶ Nucleoside analogs have been previously entrapped in CH microparticles with good entrapment efficiencies, for example cytarabine at 70.6–65%.²⁰ However, larger particles (greater than 1 μm) are not optimal for oral or IV delivery. Nucleoside analogs have also been incorporated into nanoparticles made of other biodegradable polymers, typically polyesters such as PLGA where the EE reached was as high as 78%.²¹ One of the limitations of polymeric nanoparticles is that many are made using processes that are incompatible with the nucleotide analogs. Although the EE of CH nanoparticles made in this study result in somewhat lower EEs than in other materials, the ease of preparation and use of mild conditions (moderate temperatures and nontoxic solvents) indicate that this type of entrapment still has potential usefulness, particularly if the EE can be improved.

The ionically crosslinked nanoparticles released ~38% of cladribine at 30 h. The release profile is biphasic—consisting of an initial early release phase, followed by a plateau, and a later release phase. We hypothesize that the two phases of release are attributed to initial diffusion of cladribine from the nanoparticles followed by erosion of the nanoparticle matrix thus releasing the remaining entrapped cladribine.²⁰ TEM micrographs of incubated particles show a significant decrease in nanoparticle size over the 100 h release time frame, supporting this hypothesis. Biphasic release has been observed in nucleoside analog release from PLGA microspheres, which is another biodegradable polymer.²² Modeling can help to elucidate the mechanism of drug release. The modeling results shown here support the hypothesis that the initial release phase of the ionically crosslinked nanoparticles is diffusion (n near 0.45) with the second phase being nondiffusion ($n > 1$).

The crosslinked nanoparticles had a less distinctive early release phase, with less than 10% of cladribine released at the 30-h time point (both genipin and glyoxal). Some entrapped cladribine may have diffused out of the particles during the 2 h crosslinking step, although the 100% total release from the glyoxal crosslinked particles suggests not. Crosslinking the matrix could delay or completely hinder diffusion—controlled release of cladribine by reducing the pore size of the matrix and any bead swelling that may contribute to release. Typically, covalently crosslinked CH matrices experience less swelling compared with uncrosslinked CH reducing diffusion—controlled release of entrapped molecules. The literature shows that genipin crosslinked CH has a slower degradation rate than uncrosslinked CH,⁷ which is consistent with our observations.

Very few research studies investigating controlled release of cladribine have been identified. Van Axel Castelli et al.²³ formulated cladribine with cyclodextrin to improve the solubility of the drug and develop an oral formulation. Kryczka et al.²⁴ did entrap cladribine into lactide-caprolactone or lactide-glycolide polymer films, which were then dried. The release of drug into a stationary medium measured over 50 days showed an almost-

linear release profile, which is desirable. However, the results cannot be directly compared with the results shown in this study, as the dried matrix and stationary release medium would both add to the release time. However, the Kasperczyk study indicates that drying the nanoparticles may potentially extend the release time of the cladribine, which may be appropriate for situations where longer release times are required.

A major goal of drug delivery is to achieve a long term, sustained release and minimize any burst effect. The crosslinked nanoparticles were very effective in modulating the initial diffusion—controlled release responsible for the burst effect, while providing a more gradual release in the second release phase.

CONCLUSIONS

A two-phase drug release profile was observed for all CH nanoparticles. The first phase from ionically crosslinked nanoparticles showed that 38% of the entrapped cladribine was released in the first 400 min. The initial release from the covalently crosslinked nanoparticles was much lower, and 100% of the entrapped cladribine was released from the ionically crosslinked and glyoxal-crosslinked nanoparticles after 100 h. The second release phase from genipin-crosslinked nanoparticles reached 43% of the initially entrapped cladribine, suggesting that some cladribine might still be entrapped in the CH matrix after 100 h. The release profile from the genipin-crosslinked CH nanoparticles indicated a steady, sustained release that is desirable for a cladribine DDS. The genipin-crosslinked nanoparticles may be useful for IV delivery of cladribine and other nucleotides, as the slower and more controlled release rate would allow a lower overall dose to be administered in comparison with the current requirement for large bolus IV doses that are rapidly cleared.

ACKNOWLEDGMENTS

This research was supported by funding from Natural Sciences and Engineering Research Council of Canada and the Nova Scotia Health Research Foundation. TEM facilities were provided by the Institute for Research in Materials.

REFERENCES

- Soppimath, K. S.; Aminaghavi, T. M.; Kulkarni, A. R.; Rudzinski, W. E. *J. Controlled Release* **2001**, *70*, 1.
- Vauthier, C.; Bouchemal, K. *Pharm. Res.* **2008**, *26*, 1025.
- Dodane, V.; Amin Khan, M.; Merwin, J. R. *Int. J. Pharm.* **1999**, *182*, 21.
- Thanou, M.; Verhoef, J. C.; Junginger, H. E. *Adv. Drug Deliv. Rev.* **2001**, *52*, 117.
- Juliusson, G.; Liliemark, J. *Lancet* **1993**, *341*, 54.
- Vinogradov, S. *Expert Opin. Drug Deliv.* **2007**, *4*, 5.
- Mi, F. L.; Tan, Y. C.; Liang, H. C.; Huang, R. N.; Sung, H. W. *J. Biomater. Sci. Polym. Edn.* **2001**, *12*, 835.
- Zhang, H.; Oh, M.; Allen, C.; Kumacheva, E. *Biomacromolecules* **2004**, *5*, 2461.
- Albertioni, F.; Pettersson, B.; Reichelova, V.; Juliusson, G.; Liliemark, J. *Ther. Drug Monit.* **1994**, *16*, 413.
- Denkbass, E. B.; Ottenbrite, R. M. *J. Bioact. Compat. Polym.* **2006**, *21*, 351.
- Sung, H.; Huang, R.; Huang, L.; Tsai, C. *J. Biomater. Sci. Polym. Ed.* **1999**, *10*, 63.
- Muzzarelli, R. *Carbohydr. Polym.* **2009**, *77*, 1.
- Ritger, P.; Peppas, N. *J. Controlled Release* **1987**, *5*, 23.
- Ritger, P.; Peppas, N. *J. Controlled Release* **1987**, *5*, 37.
- Kim, D. G.; Jeong, Y. I.; Choi, C.; Roh, S. H.; Kang, S. K.; Jang, M. K.; Nah, J. W. *Int. J. Pharm.* **2006**, *319*, 130.
- Wang, C.; Fu, X.; Yang, L. *Chin. Sci. Bull.* **2007**, *52*, 883.
- Win, K. Y.; Feng, S. S. *Biomaterials* **2005**, *26*, 2713.
- Vila, A.; Sanchez, A.; Tobio, M.; Calvo, P.; Alonso, M. J. *J. Controlled Release* **2002**, *78*, 15.
- Janes, K. A.; Alonso, M. J. *J. Appl. Polym. Sci.* **2003**, *88*, 2769.
- Blanco, M. D.; Gomez, C.; Olmo, R. *Int. J. Pharm.* **2000**, *202*, 29.
- Diab, R.; Degobert, G.; Hamoudeh, M.; Dumontet, C.; Fessi, H. *Expert Opin. Drug Deliv.* **2007**, *4*, 513.
- Cifti, K.; Hincal, A. A.; Kas, H. S.; Ercan, T. M.; Sungur, A.; Guven, O.; Ruacan, S. *Pharm. Dev. Technol.* **1997**, *2*, 151.
- Van Axel Castelli, V.; Trivieri, G.; Zucchelli, I.; Brambilla, L.; Barbuzzi, T.; Castiglioni, C.; Paci, M.; Zerbi, G.; Zanol, M. *J. Pharm. Sci.* **2008**, *97*, 3897.
- Kryczka, T.; Bero, M.; Kasperczyk, J.; Dobrzynski, P.; Marciniak, B.; Popielarz-Brzezinska, M.; Grieb, P. *Acta Biochim. Pol.* **2002**, *49*, 205.